MINERALOGICAL MAGAZINE, SEPTEMBER 1975, VOL. 40, PP. 239–45

Thermal transformation of lepidomelane

MIZUHIKO AKIZUKI, HIROSHI KONNO, NORIYOSHI YAMAUCHI, AND ICHIRO SUNAGAWA

Institute of Mineralogy, Petrology and Economic Geology, Faculty of Science, Tohoku University, Sendai, 980 Japan

SUMMARY. Lepidomelane, an iron-rich biotite, was heated in air or in vacuum, or by electron bombardment, and the processes of dehydration and transformation were studied by means of X-ray diffractometry, optical microscopy, and electron microscopy. By heat treatment, vacancies are at first formed by the evaporation of water molecules and alkali ions, and they move and condense to form holes, which act as preferential nucleation sites for new phases. Other preferential sites are edges of exposed silicate sheets along microcracks, and these are decorated by a newly formed maghemite-like mineral whose a is 10·20 Å (on a hexagonal cell), so that the sites can be clearly seen even under the reflection microscope. By heating at higher temperatures or prolonged heating, various phases, olivine, hematite, magnetite, and leucite are formed, depending upon the conditions of dehydration.

DEHYDRATION and crystallization processes taking place in various hydrated silicates have attracted great interest in recent years. The transmission electron-microscopic technique has been applied to the examination of the process of thermal transformation of these minerals. Nakahira (1965, 1966) studied the process of dehydration of both muscovite and phlogopite by electron and phase-contrast microscopy and discussed the differences of dehydration processes between the two minerals. Since it is not necessary to take oxygen in air into consideration in Nakahira's cases of iron-poor muscovite and phlogopite, other components were not added to the starting material, and only water molecules were removed during the process. In contrast, in the thermal transformation of muscovite in molten KCl (Akizuki *et al.*, 1972), other components were added to the starting material.

For an iron-rich mineral such as lepidomelane, if the specimen is heated in air, the transformation process should be essentially different from that of iron-poor minerals. Therefore, we set out to investigate by means of X-ray diffractometry and optical and electron microscopy the process and the products of transformation, when iron-rich biotite, lepidomelane, is heated in air and in vacuum and by electron bombardment, and tried to find the essential differences under different conditions.

As to heating experiments of biotite, several previous works may be mentioned, such as by Walker (1940), Roy (1949), Grim and Bradley (1940). In these studies dehydration products are described but the transformation processes were not studied. In the present study the main attention was paid on the process of transformation and on the preferential sites for nucleation of new phases.

Specimen and method. The material used is a dark-green lepidomelane from

[1] Present address: Nippon Toki Co., Nagoya, Japan.

Kawamata pegmatite, Fukushima Pref., Japan. The chemical composition is shown in Table I.

Specimens were heated in air or in vacuum or by electron bombardment in the electron microscope. Then the former two specimens were observed under both reflection optical and electron microscopes, and the latter under the electron microscope only. The specimens heated at higher temperature than about 1000 °C were too tightly sintered to be observed under the electron microscope, and so were studied only by means of X-ray diffractometry.

TABLE I. *Chemical composition of lepidomelane from Kawamata pegmatite, Japan. (Analyst H. Konno)*

	wt %		O(OH) = 24				
SiO_2	31·50	Si	5·16	8·00	CaO	None		
TiO_2	2·45	Al	2·84		Na_2O	0·15	Na	0.05	1·54
		Al	0·04		K_2O	7·13	K	1·49	
Al_2O_3	14·96	Ti	0·30		H_2O^+	3·33	OH	3·63	
Fe_2O_3	10·77	Fe^{3+}	1·32	5·87	H_2O^-	1·41	O	20·37	
FeO	24·00	Fe^{2+}	3·28						
MnO	0·72	Mn	0·10		Total	99·77			
MgO	3·40	Mg	0·83						

Results. The dehydration curve in air is similar to that of Roy (1949), except that a small endothermic peak appears between 400 and 500 °C. The d_{001} dimension was measured using the 006 reflection during heating in air. For the starting material it is 20·11 Å at room temperature; then it increases gradually up to 20·20 Å at 375 °C. It starts to decrease from 375 °C, and becomes 20·03 Å at 450 °C. Henceforth, it again increases gradually and reaches to 20·18 Å at 940 °C. The dimension decreases to 19·83 Å when the sample is cooled down to room temperature, though the volume of the specimen expands slightly due to dehydration. The specimen heated in air below about 1000 °C for 12 hours does not show any distinct new phases on the X-ray chart. On further heating at 1100 °C for 3·5 hours the lepidomelane decomposes and transforms completely into hematite and leucite.

When the specimen sealed in a small evacuated tube of silica glass is heated at 700 °C for 42 hours and at 1100 °C for 3·5 hours, strong diffraction peaks of both magnetite and leucite and weak peaks of fayalite are recorded on X-ray charts.

Slices freshly cleaved from the specimen and heated at 500 °C in air do not show any distinct changes under the reflection optical microscope, except that the outermost surface is coloured red due to newly formed hematite on the surface. However, when the slices are investigated under the electron microscope it is found that there are a large number of minute elongate hexagonal holes, 700 to 800 Å in elongation. The density of the holes increases with the heating temperature. Some dislocation lines are pinned by these holes, around which strain fields are seen (fig. 1). It is considered that these holes played a role of pinning for the movement of dislocations, and not

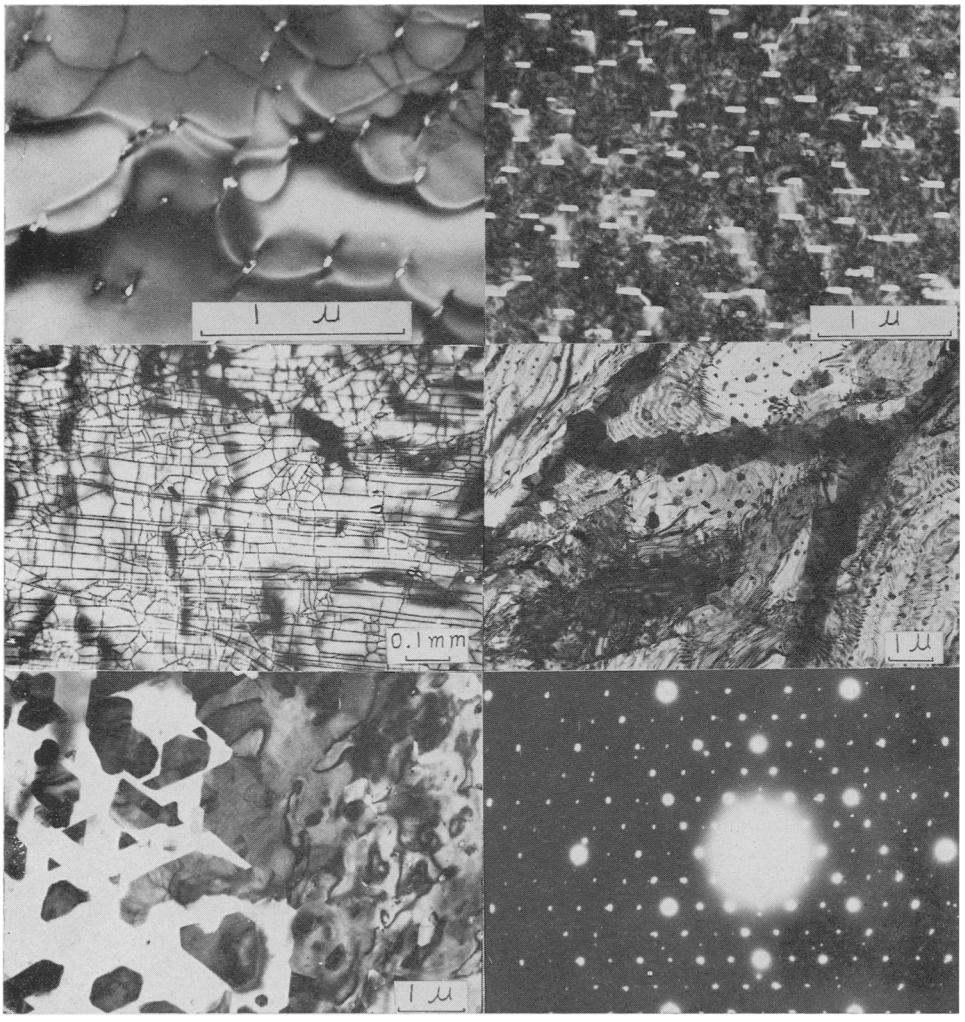

FIGS. 1 to 6: FIG. 1 (top left). Electron microphotograph showing dislocations pinned by holes. FIG. 2 (top right). Electron microphotograph showing hexagonal holes and complicated diffraction contrasts around them. FIG. 3 (middle left). Reflection optical microphotograph showing microcracks decorated by maghemite-like phase. The *b*-axis is horizontal. FIG. 4 (middle right). Electron microphotograph showing maghemite-like mineral precipitated along the cracks of lepidomelane. FIG. 5 (bottom left). Electron microphotograph showing maghemite-like mineral. See text for detail. FIG. 6 (bottom right). Electron diffraction pattern of maghemite-like mineral.

vice versa. Complicated diffraction contrasts and many small newly formed phases are seen on slices with a high density of holes (fig. 2).

Specimens heated in air at temperatures from 600 to 900 °C for 2 to 24 hours show iridescence and exhibit irregular net-work patterns in which parallel lines elongated in the direction of *b*-axis predominate (fig. 3). Under the electron microscope the specimens show many small hexagonal, triangular, or trapezoidal platy crystals preferentially formed along microcracks, though a few distribute randomly on the surface (fig. 4). Fig. 5 offers a clear view of these newly formed platy crystals. It is seen that some are twinned, with the twinning boundary parallel to one edge of the crystal. In fig. 5, the white area on the left is the fresh lepidomelane that has not been decomposed. Hexagonal or triangular thin plates seen in this area are the newly formed crystals on this surface. On the right, such newly formed crystals coalesce together and form a thin continuous layer. On the extreme right one may see a somewhat wavy and irregular surface. This is a sort of transformation front, and further right we can find a fresh lepidomelane surface. Thus, fig. 5 shows an area where transformation is actually taking place.

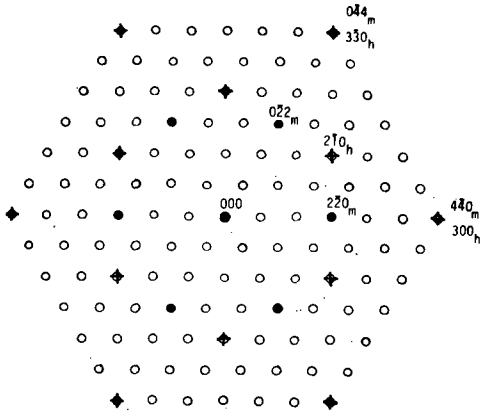

FIG. 7. Schematical electron diffraction pattern of fig. 6: open circle, maghemite-like mineral; solid circle, magnetite; cross, hematite.

An electron-diffraction pattern of the newly formed phase in the specimens heated in air at 850 °C is shown in fig. 6, on which diffraction spots from lepidomelane are not superimposed. The pattern is schematically shown in fig. 7, together with the spots of hematite and magnetite. From the electron diffraction, $a = 10{\cdot}20$ Å in a trigonal primitive cell is computed, and this value corresponds to $\sqrt{6}/2$ times a of magnetite, and also to twice a of hematite. Several attempts were made to increase the amount of this phase by heating the specimens for longer times and at higher temperatures, hoping that the phase might be formed in sufficient quantity for X-ray diffractometry, but without success. Instead of obtaining more of the new phase, the amount of hematite increased with increasing temperatures and times.

When the specimen is heated in vacuum olivine, magnetite, and leucite are formed. The phase observed above was not found in this case. The olivines are large and thin and can be observed directly under the electron microscope (fig. 8), but not magnetite or leucite; the olivine is most probably fayalite. The crystallographic relations between lepidomelane (lep) and fayalite (fa) are: $[100]_{lep} \parallel [010]_{fa}$, $[010]_{lep} \parallel [001]_{fa}$, and

$$2a(2\times 5{\cdot}3\ \text{Å})_{lep} = b(10{\cdot}5\ \text{Å})_{fa},\ 2b(2\times 9{\cdot}2\ \text{Å})_{lep} = 3c(3\times 6{\cdot}1\ \text{Å})_{fa}.$$

Some of the larger crystals of leucite and magnetite can be seen under the optical

microscope. We were unable to detect any relation between these and micro cracks in lepidomelane, either under the optical or the electron microscope.

When the lepidomelane is bombarded by electron beams under the electron microscope the diffraction pattern changes abruptly. At an early stage of bombardment diffraction spots corresponding to a spinel phase and spots similar to fig. 6, but weaker, start to appear together with the spots from lepidomelane. The spots from lepidomelane gradually fade away with increasing electron density and the spots from a spinel phase become strong; then those from olivine start to appear, but the spots similar to fig. 6 disappear. Finally, the spots consisting of the mixture of the spinel phase (magnetite) and olivine (fayalite) are formed. In this case no close relation between the sites of new phases and microcracks or holes in lepidomelane, such as was observed in the case of heat treatment in air, was noticed. The orientational relations between the host lepidomelane and the new phases are: $[001]_{lep} \parallel [111]_{sp}$, $[010]_{lep} \parallel [110]_{sp}$, $[110]_{sp} \parallel [001]_{fa}$, $[112]_{sp} \parallel [010]_{fa}$, where the suffix sp connotes spinel phase.

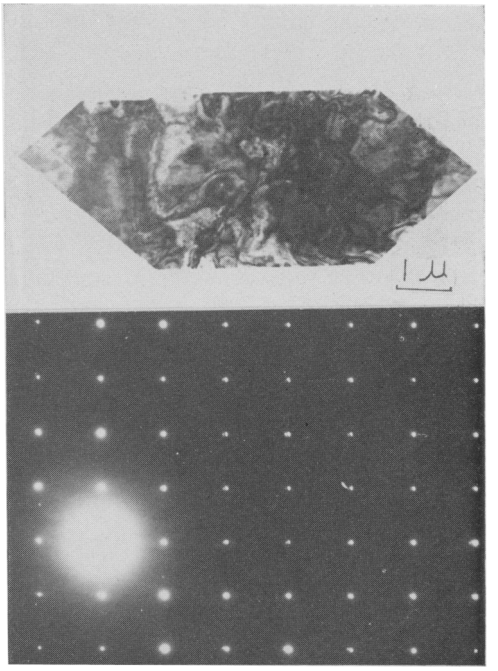

FIG. 8. Electron microphotograph and electron diffraction of olivine. c and c^* axes are horizontal.

Discussion. When lepidomelane is heated in air, at first many holes are formed. Although they occasionally relate with dislocations, as shown in fig. 1, they are more commonly formed at random positions or along the b-axis (fig. 2). These holes are considered to have been formed through somewhat complicated processes: the first stage is perhaps the escape of alkali ions and water molecules from point defects; in order to reduce the total strain energy around these minute holes formed at first, they have to migrate through the crystal and coalesce together to form clusters of holes of larger sizes; in order to maintain the electrical neutrality, other ions will also migrate through the crystal or will be exsolved along certain defects, and these will also result in the formation of holes.

The periphery of the holes is the exposed edges of the silicate sheets. This will act as a preferential site where oxygen atoms migrating through the crystal due to dehydration can preferentially react with the host crystal to form new phases. It is indeed observed that there is a close relation between holes and newly formed phases (fig. 2). Similar exposed edges of the silicate sheets may be expected along the steps created by microcracks inclined to the cleavage face in the host crystal. This is

witnessed by the fact that the microcracks are heavily decorated by the newly formed phase (fig. 3, 4). Since similar microcracks are seen under the electron microscope even in the untreated specimens, at least some of them must have existed from the beginning, and some were created during heating. The decorated net-work patterns (fig. 3) should correspond to this sort of microcrack.

Although Champness (1970) reported on olivine crystals that dislocations in the host crystal play an important role as preferential nucleation sites for the newly formed phases, this was not observed in the present case. More important sites in the case of lepidomelane are exposed edges of silicate sheets due to the formation of holes or microcracks.

The phase shown in figs. 6 and 7, which is too small to be analysed by means of electron-probe microanalyser, is considered to be an iron oxide, because it changes into hematite after prolonged heating.

Recently, Kokhanchik and Serebryakov (1973) have studied Al_2O_3 in internally oxidized Cu–Al alloys, which have simple compositions, and found at least five different types of electron diffraction patterns, one of which is very similar to the pattern in figs. 6 and 7. They found the pattern to be a super-structure of spinel-type γ-Al_2O_3 with a trigonal primitive lattice. The difference between the five types is associated with different dispositions of cations in the tetrahedral vacancies of the spinel lattice of Al_2O_3. Since in the case of Al_2O_3 the number of cations in the tetrahedral vacancies is one-third less than that of spinel, there will be four cations instead of six for the same method of filling the (111) planes in Al_2O_3. Common maghemite can be explained in terms of the ordering of the tetrahedral vacancies in the direction of [111]; however, the electron-diffraction pattern in figs. 6 and 7 cannot be explained by this method of ordering, nor by the structure of β-Fe_2O_3, which was found in the process of phase transition from hematite to maghemite (Finch and Sinha, 1957). The pattern can be accounted for if the arrangement of the atoms in the (111) planes of the spinel is changed; therefore, the present crystal is conjectured to belong to maghemite group, having the same superstructure as the spinel-type γ-Al_2O_3 of Kokhanchik *et al.*, though its chemical composition has not been analysed.

The orientation relation between the spinel cell and the cell of the maghemite-like mineral is shown in fig. 7 and is: $(111)_{sp} \parallel (001)_{maghemite}$; $[0\bar{1}1]_{sp} \parallel [010]_{maghemite}$.

At high temperatures hematite is stably formed in air and magnetite in vacuum. It is considered that the maghemite-like mineral is formed in the process of suitable oxidation of iron in lepidomelane. If oxygen pressure has been fully controlled during the transformation, it is expected that the maghemite-like mineral might be formed in quantity at higher temperatures under intermediate oxygen pressure. Further studies are desirable.

One more comment to be added is that olivine crystals grow large when lepidomelane is sealed in a silica tube, whereas they are electron microscopically minute when the water is constantly removed from the silica tube by pumping. It is well known that even a small amount of water can act as a good mineralizer to grow larger crystals, and the present case serves as further evidence for that.

REFERENCES

AKIZUKI (M.), SATO (S.), and SUNAGAWA (I.), 1972. *Min. Journ.* **6**, 448.
CHAMPNESS (P. E.), 1970. *Min. Mag.* **37**, 790.
FINCH (G. I.) and SINHA (K. P.), 1957. *Proc. Roy. Soc.* A**241**, 1–8 [M.A. **14**–100].
GRIM (R. E.) and BRADLEY (W. F.), 1940. *Journ. Amer. Ceram. Soc.* **23**, 242 [M.A. **8**–295].
[KOKHANCHIK (G. I.) and SEREBRYAKOV (A. V.)] Коханчик (Г. И.) и Серебряков (А. Б.), 1973. Кристаллография (*Kristallografiya*) **18**, 741.
NAKAHIRA (M.), 1965. *Amer. Min.* **50**, 1432 [M.A. **17**–562].
—— and UDA (M.), 1966. Ibid. **51**, 454 [M.A. **17**–737].
ROY (R.), 1949. *Journ. Amer. Ceram. Soc.* **32**, 202.
WALKER (G. F.), 1940. *Min. Mag.* **28**, 693.

[*Manuscript received 29 July 1974*]